FERMILAB-CONF-14-191-AD-APC-ESH-FESS
June 2014

TARGET STATION DESIGN FOR THE MU2E EXPERIMENT*†

V.S. Pronskikh, G. Ambrosio, M. Campbell, R. Coleman, G. Ginther, V. V. Kashikhin, K. Krempetz, M. Lamm, A. Lee, A. Leveling, N. V. Mokhov, V. P. Nagaslaev, A. Stefanik, S. Striganov, S. Werkema
Fermi National Accelerator Laboratory, Batavia, IL 60510, USA
L. Bartoszek
Bartoszek Engineering, Aurora, IL, USA
C. Densham, P. Loveridge
Rutherford Appleton Laboratory, UK
K. Lynch, J. Popp
York College at CUNY, New York, USA

Abstract

The Mu2e experiment at Fermilab is devoted to search for the conversion of a negative muon into an electron in the field of a nucleus without emission of neutrinos. One of the main parts of the Mu2e experimental setup is its Target Station in which negative pions are generated in interactions of the 8-GeV primary proton beam with a tungsten target.A large-aperture 5-T superconducting production solenoid (PS) enhances pion collection, and an S-shaped transport solenoid (TS) delivers muons and pions to the Mu2e detector. The heat and radiation shield (HRS) protects the PS and the first TS coils. A beam dump absorbs the spent beam. In order for the PS superconducting magnet to operate reliably the sophisticated HRS was designed and optimized for performance and cost. The beam dump was designed to absorb the spent beam while maintaining its temperature and air activation in the hall at the allowable level. Comprehensive MARS15 simulations have been carried out to optimize all the parts while maximizing muon yield. Results of simulations of critical radiation quantities and their imply cations on the overall Target Station design and integration are discussed.

* Work supported by Fermi Research Alliance, LLC under contract No. DE-AC02-07CH11359 with the U.S. Department of Energy.
† Presented at the 5th International Particle Accelerator Conference IPAC14, June 15-20, 2014, Drezden, Germany
# vspron@fnal.gov

TARGET STATION DESIGN FOR THE MU2E EXPERIMENT *

V.S. Pronskikh, G. Ambrosio, M. Campbell, R. Coleman, G. Ginther, V. V. Kashikhin, K. Krempetz, M. Lamm, A. Lee, A. Leveling, N. V. Mokhov, V. P. Nagaslaev, A. Stefanik, S. Striganov, S. Werkema, Fermi National Accelerator Laboratory, Batavia, IL 60510, USA
L. Bartoszek, Bartoszek Engineering, Aurora, IL, USA
C. Densham, P. Loveridge, Rutherford Appleton Laboratory, UK
K. Lynch, J. Popp, York College at CUNY, New York, USA

Abstract

The Mu2e experiment at Fermilab is devoted to search for the conversion of a negative muon into an electron in the field of a nucleus without emission of neutrinos. One of the main parts of the Mu2e experimental setup is its Target Station in which negative pions are generated in interactions of the 8-GeV primary proton beam with a tungsten target. A large-aperture 5-T superconducting production solenoid (PS) enhances pion collection, and an S-shaped transport solenoid (TS) delivers muons and pions to the Mu2e detector. The heat and radiation shield (HRS) protects the PS and the first TS coils. A beam dump absorbs the spent beam. In order for the PS superconducting magnet to operate reliably the sophisticated HRS was designed and optimized for performance and cost. The beam dump was designed to absorb the spent beam while maintaining its temperature and air activation in the hall at the allowable level. Comprehensive MARS15 simulations have been carried out to optimize all the parts while maximizing muon yield. Results of simulations of critical radiation quantities and their implications on the overall Target Station design and integration are discussed.

INTRODUCTION

The Mu2e Production Target Station (Figure 1) consists of five components: the pion production target, the remote handling system to change targets, the production solenoid heat and radiation shield (HRS), the proton beam absorber, and the protection collimator. The remote handling area is used to store the target change robot. The Production Solenoid (PS) hatch consists of a stack of shielding blocks that can be removed to allow access with an external crane. The proton beam absorber is unmovable and part of the concrete structure of the building.

PRODUCTION TARGET

The production target generates pions that decay to muons as they are transported in the backward direction to the stopping target in the detector solenoid. The target will be installed inside the bore of the production solenoid within a graded magnetic field, a configuration designed to maximize the production and capture of low-energy negative pions generated by interaction with the 8 GeV primary proton beam.

* Work supported by Fermi Research Alliance, LLC, under contract No. DE-AC02-07CH11359 with the U.S. Department of Energy.

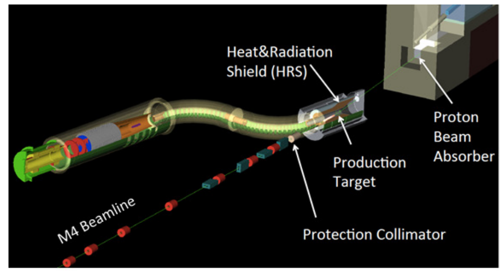

Figure 1: Target station layout.

Pion production is maximized with a dense, high atomic number material to ensure a high rate of beam-target interactions. A compact target geometry is used to minimize pion reabsorption. The refractory metal tungsten is optimal, since at the design beam power of 8 kW it will be able to directly radiate the generated heat load to the solenoid shield without the need for a coolant. The target operating temperature distribution is shown in Figure 2.

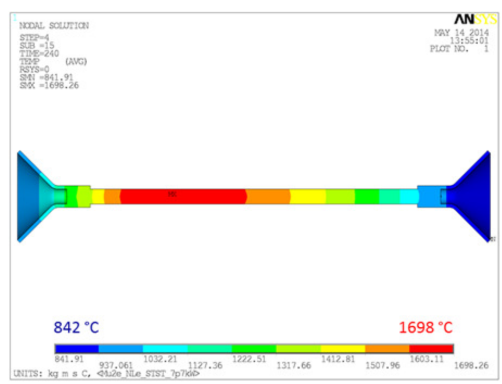

Figure 2: Target steady-state operating temperature assuming a heat load of 560 W and temperature dependent literature values for thermal emissivity.

Target Remote Handling

The Mu2e target remote handling system provides a means to remove the downstream production solenoid window and the target, dispose of them both, and replace them with new components. A remote means of accomplishing these tasks is required because of the high radiation environment in and around the production solenoid after beam operations. The system utilizes a robotic chassis mounted to floor rails. On board the robotic chassis are servo-positioning X, Y, and dual Z-axes. After the shielding door is opened, the robot travels from the remote handling room out into the target hall on a floor rail / linear drive system. Once the robot is in position behind the production solenoid, a pneumatic brake is engaged to hold it in place, and the remote handling room door can be closed while the robot completes its tasks. Also included in the remote handling system are a staging frame (in the Remote Handling Room, which holds the new target and window), and the waste storage cask (in the target hall, which holds the old targets and PS access windows). Total target replacement time will be approximately 4 weeks.

HEAT AND RADIATION SHIELD

HRS serves to protect the superconducting coils of PS from the intense heat and radiation generated by the primary (8 kW) 8 GeV kinetic energy proton beam striking the production target within the evacuated warm bore of the PS. The shield also protects the coils in the far upstream end of the transport solenoid (TS), a straight section of coils, called TS1, at the exit to the PS. The HRS shields downstream components from neutron and gamma background.

There are four primary performance parameters for HRS (see [1] for details): 1) The total allowed dynamic, i.e., instantaneous, heat load in the magnet coils, 2) The local peak power density in the superconducting coils, 3) The maximum local radiation dose to the superconductor insulation and epoxy over the lifetime of the experiment, 4) The radiation damage to the PS superconductor's aluminum stabilizer and copper matrix. HRS has sufficient inner aperture (20 cm in radius) to allow good capture of pions and muons to maximize the stopping rate of negative muons in the detector solenoid stopping target. In addition, the shield design avoids any line-of-sight cracks between components that point from the target to the PS inner cryostat wall and thus the magnet coils. The materials used to construct the shield will not cause the magnetic field of PS to fall outside of specifications. This implies the use of non-magnetic materials with a magnetic permeability of less than 1.05.

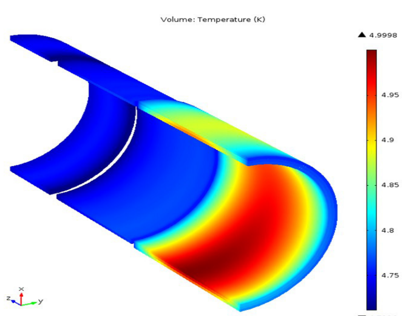

Figure 3: Peak PS coil temperature.

The HRS design has evolved over time based on numerous studies using MARS15 [2] and because interface requirements. The model of the PS+HRS geometry is shown in Figure 5. Extensive variations have been explored in both geometry and materials. Most recently the effect on the HRS design on the neutron and gamma backgrounds downstream of the production solenoid have also been considered.

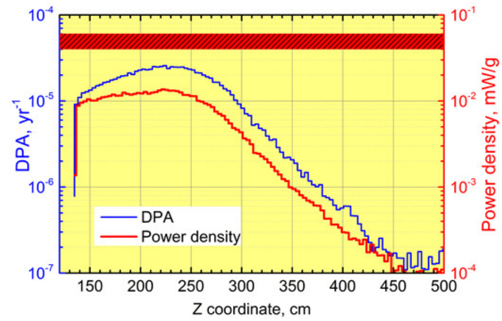

Figure 4: The MARS results for the peak DPA and peak power density at the PS coils.

HRS requires active cooling. The simplest and most reliable solution is to flow water around the entire HRS in tank. The HRS design includes a stainless steel liner that isolates the HRS volume, including the cooling water, from both the solenoid and the beamline vacuum. The water also provides good shielding for low-energy neutrons and gammas that are a source of noise in the cosmic ray veto (CRV) detector.

Materials used to construct HRS [3] (bronze and water) do not cause the magnetic field of the Production Solenoid to fall outside of specification, therefore, non-magnetic ones are used. All conducting materials are designed to reduce eddy current forces that might develop during a quench. Bronze C63200 satisfies these requirements and is the material of choice. It can also be manufactured in large forged pieces, simplifying assembly. Table 1 summarizes the requirements to the radiations quantities for the PS coils as well as the HRS performance (see also [3] for details). The temperature distribution in PS magnet coils (NbTi with Al stabilizer) is shown in Figure 3. Simulated power density and DPA damage in the coil stripe closest to the beam exit is shown in Figure 4. A section view of the HRS model based on the design studies described above is given in Figure 5. The DPA limit for the TS coil nearest to PS is $\sim 10^{-5}$ yr^{-1}, and the simulated level is significantly lower.

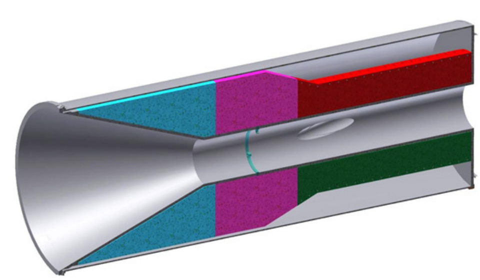

Figure 5: Section view of HRS. Bronze pieces are shown in light blue, purple and red. A stainless steel liner surrounds the bronze on all sides and the vessel holds 600 gallons of water.

Table 1: Performance of HRS compared to specifications on the magnet coils.

	Peak DPA/yr*10^{-5},	Peak power density, μW/g	Absorbed dose, MGy/yr	Dynamic heat load, W
Specification	4 to 6	30	0.35	100
Performance	2.4	13	0.26	24

PROTON BEAM ABSORBER

The Mu2e beam absorber stops the unspent proton beam and secondary particles that make their way through and beyond the target in the forward direction. The beam power from the accelerator complex is 8 kW, and while 0.7 kW will be deposited into the target itself, and 3.3 kW will be absorbed by PS and HRS, a significant amount of power is deposited in the beam absorber. The beam absorber will be shielded so that its prompt and residual radioactivity does not significantly contribute to the radiation dose rate at the downstream end of the production solenoid enclosure.

The absorber will be able to accept the entire beam power in the event of the target missed, or during pre-targeting beam tests. The beam absorber will be placed outside of and well beyond PS to allow access to the crane hatch and room for remote target exchange equipment; it is compatible with the extinction monitor located above and behind the beam absorber.

The beam absorber will be able to accept the total number of protons required by the experiment, $3.6 \cdot 10^{20}$ over 3-4 years, plus an acceptable overhead to account for commissioning and tuning (100%), without replacement over the life of the experiment. The transverse dimensions of the absorber is consistent with the beam properties after accounting for distance from the target and divergence of the beam, including scattering in the target. The transverse proton beam size at the absorber face has a dispersion of 1.3 cm in both planes.

The absorber consists of a steel core with the dimensions $1.5 \times 1.5 \times 2$ m and concrete shielding with the dimensions $3.5 \times 3.5 \times 5$ m, so the core is surrounded by 1 m of concrete on the sides, the top, and the bottom. It has a 1.5×1.5 m opening toward the beam and also a $2.5 \times 2.5 \times 1$ m albedo trap to protect the downstream end of PS from the secondary particles generated by the spent proton beam in the core. Figure 6 shows the temperature distribution in the beam absorber.

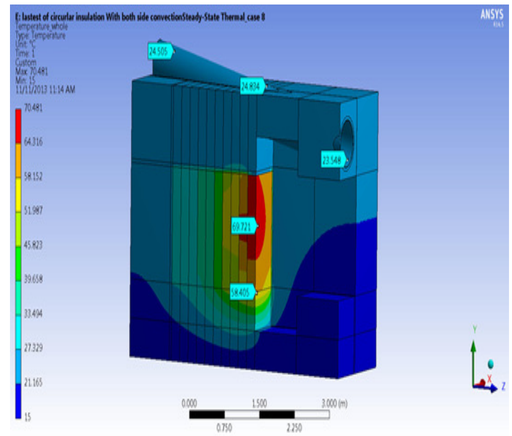

Figure 6: Temperature distribution in the absorber steel and shielding concrete for normal operation.

PRODUCTION SOLENOID PROTECTION COLLIMATOR

Normally, proton beam will interact with the production target located within the PS bore, with the remnant beam delivered to the proton beam absorber located well downstream of the production region. There are stringent limits for heat loads on components of the entire system. In addition, there are also stringent limits on displacements per atom (DPA) for the aluminum-stabilized superconductor in PS. In particular, beam accident conditions that result in direct interaction of primary beam protons with HRS, cryostat walls, or coils, could result in significant heat deposition or radiation damage to these components.

During beam accident conditions, the protection collimator (PC) will be able to absorb and dissipate the heat load from the full primary beam for at least 50 msec before the beam protection systems trip off the beam. To intercept the beam in any accident condition, PC has a minimum transverse dimension of 50 cm.

During normal operations, the beam will have a transverse size within the PC aperture of $\sim$ 1 cm full-width. To maximize targeting flexibility, the beam aperture through the PC should be as wide as possible, but the requirement to limit fake signals in the extinction monitor limits the aperture diameter to 80 mm.

The pion production target is 0.6 cm in diameter, thus the beam will move transversely by 1 cm in each direction to ensure the beam can be swept across the target for targeting studies and optimization. Since the 80 mm aperture size violates the requirement to be able to swing the beam $\pm 0.8°$ about the geometric center of the target, the protection collimator must be able to move out of the proton beam within its vacuum volume.

REFERENCES

[1] V.S. Pronskikh, Modern Physics Letters A, Vol. 28, **19**, 1330014 (2013).

[2] N.V. Mokhov *et al.*, Fermilab Report Fermilab-FN-628 (1995); N.V. Mokhov *et al.*, AIP Conf. Proc. 896, pp. 50-60 (2007); http://www-ap.fnal.gov/MARS/.

[3] V.S. Pronskikh *et al.*, Nuclear Physics B (Proc. Suppl.) 248–250 (2014) 118–120.